Supplement of Hydrol. Earth Syst. Sci., 30, 3715–3739, 2026
https://doi.org/10.5194/hess-30-3715-2026-supplement

Hydrology and Earth System Sciences
Open Access
EGU

Supplement of

Exploring impacts of forest management strategies on water partitioning in a drought-sensitive catchment using a tracer-aided ecohydrological framework

Cong Jiang et al.

Correspondence to: Cong Jiang (cong.jiang@igb-berlin.de)

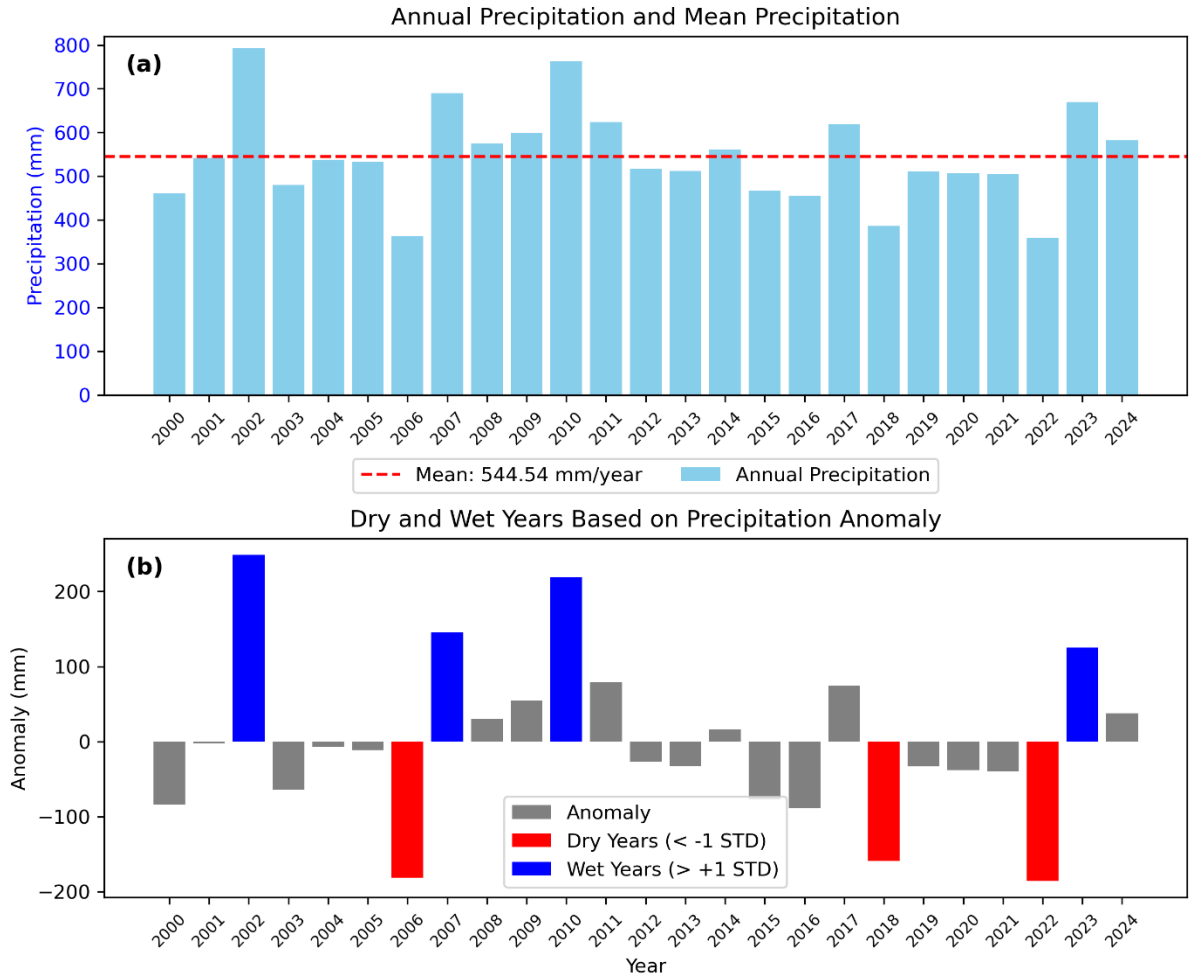

Figure S1. Annual precipitation and anomalies for the DMC. (a) Annual precipitation with the long-term mean (red dashed line). (b) Precipitation anomalies highlighting dry (red, anomaly < −1 standard deviation) and wet (blue, anomaly > +1 standard deviation) years.

Table S1. Ecohydrological processes in EcoPlot-iso: variable definitions and governing equations.

Variable	Description	Equation
SCF	Surface cover fraction	$\mathrm{SCF} = 1 - e^{(\mathrm{rE} * \mathrm{LAI})}$ (S1)
Int	Canopy interception	$\mathrm{Int} = (\alpha * \mathrm{LAI}) * \left(1 - \frac{1}{1 + \frac{\mathrm{SCF} * P}{\alpha * \mathrm{LAI}}} \right)$ (S2)
T_p	Canopy fraction of PET	$T_p = \mathrm{PET} * \mathrm{SCF}$ (S3)
E_p	Soil fraction of PET	$E_p = \mathrm{PET} * (1 - \mathrm{SCF})$ (S4)
E_i	Canopy evaporation	$E_i = \begin{cases} \mathrm{Int}_S & \text{if } T_p > \mathrm{Int}_S \\ T_p & \text{if } T_p \le \mathrm{Int}_S \end{cases}$ (S5)
E_s	Soil evaporation of upper soil layer	$E_s = E_p * \left(\frac{S_\mathrm{U}}{S_{\mathrm{U,max}}} \right)$ (S6)
T_{p1}	Transpiration from the upper soil layer	$T_{p1} = r_{L1} * (T_P - E_i) * \left(\frac{S_\mathrm{U}}{S_{\mathrm{U,max}}} \right)$ (S7)
T_{p2}	Transpiration from the lower soil layer	$T_{p2} = r_{L2} * (T_P - E_i - T_{p1}) * \left(\frac{S_\mathrm{M}}{S_{\mathrm{M,max}}} \right)$ (S8)
T_{p3}	Transpiration from the deep soil layer	$T_{p3} = r_{L3} * (T_P - E_i - T_{p1} - T_{p2}) * \left(\frac{S_\mathrm{D}}{S_{\mathrm{D,max}}} \right)$ (S9)
Q_s	Surface runoff	$Q_s = \mathrm{PN} - I_\mathrm{c}$ (S10)
Pref_Flow	Preferential flow	$\mathrm{Pref\_Flow} = \mathrm{PN} * \mathrm{PF}_{\mathrm{scale}}$ (S11)
Perc	Percolation flux	$\mathrm{Perc} = k_{\mathrm{s1}} * \left(\frac{S_\mathrm{U}}{S_{\mathrm{U,max}}} \right)^{g_1}$ (S12)
Sdeep	Compartment flow	$\mathrm{Sdeep} = k_{\mathrm{s2}} * \left(\frac{S_\mathrm{M}}{S_{\mathrm{M,max}}} \right)^{g_2}$ (S13)
Recharge	Groundwater recharge	$\mathrm{Recharge} = k_{\mathrm{s3}} * \left(\frac{S_\mathrm{D}}{S_{\mathrm{D,max}}} \right)^{g_3}$ (S14)

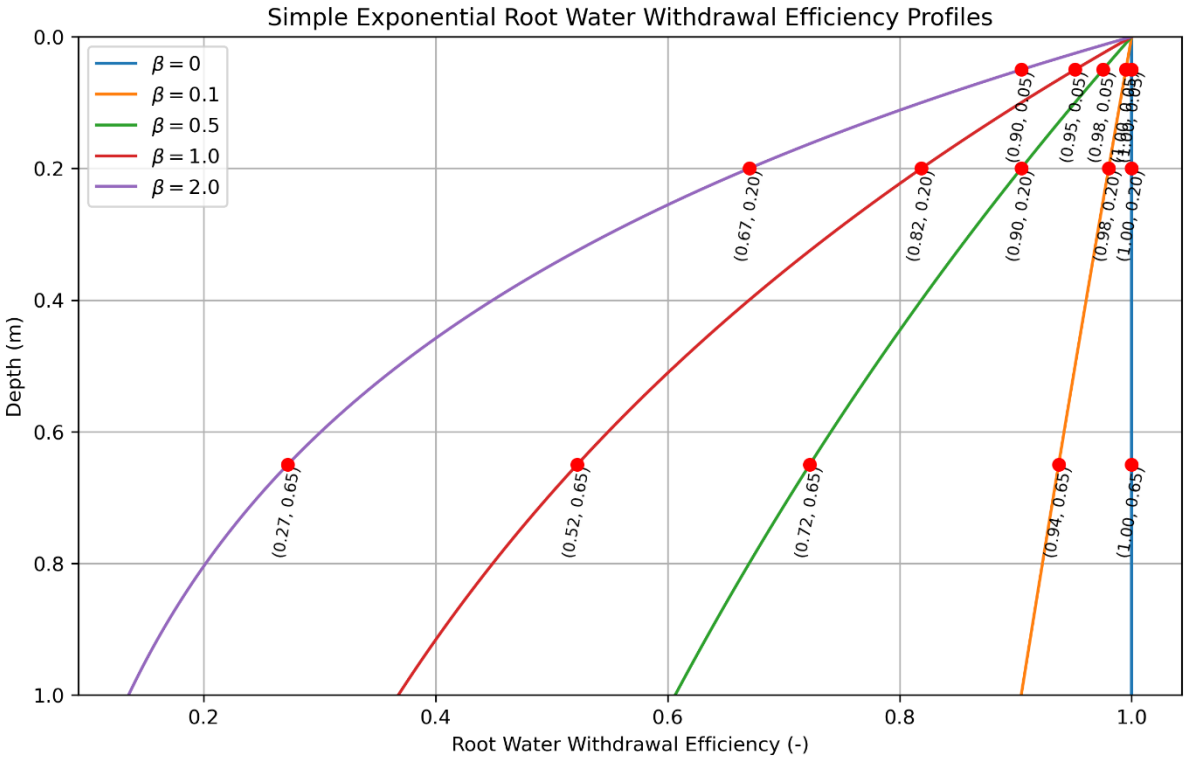

Figure S2. Exponential root water withdrawal efficiency function and profiles for different β values. β = 0 represents a deep-rooted system, while a larger β indicates a shallow-rooted system with root activity concentrated near the surface.

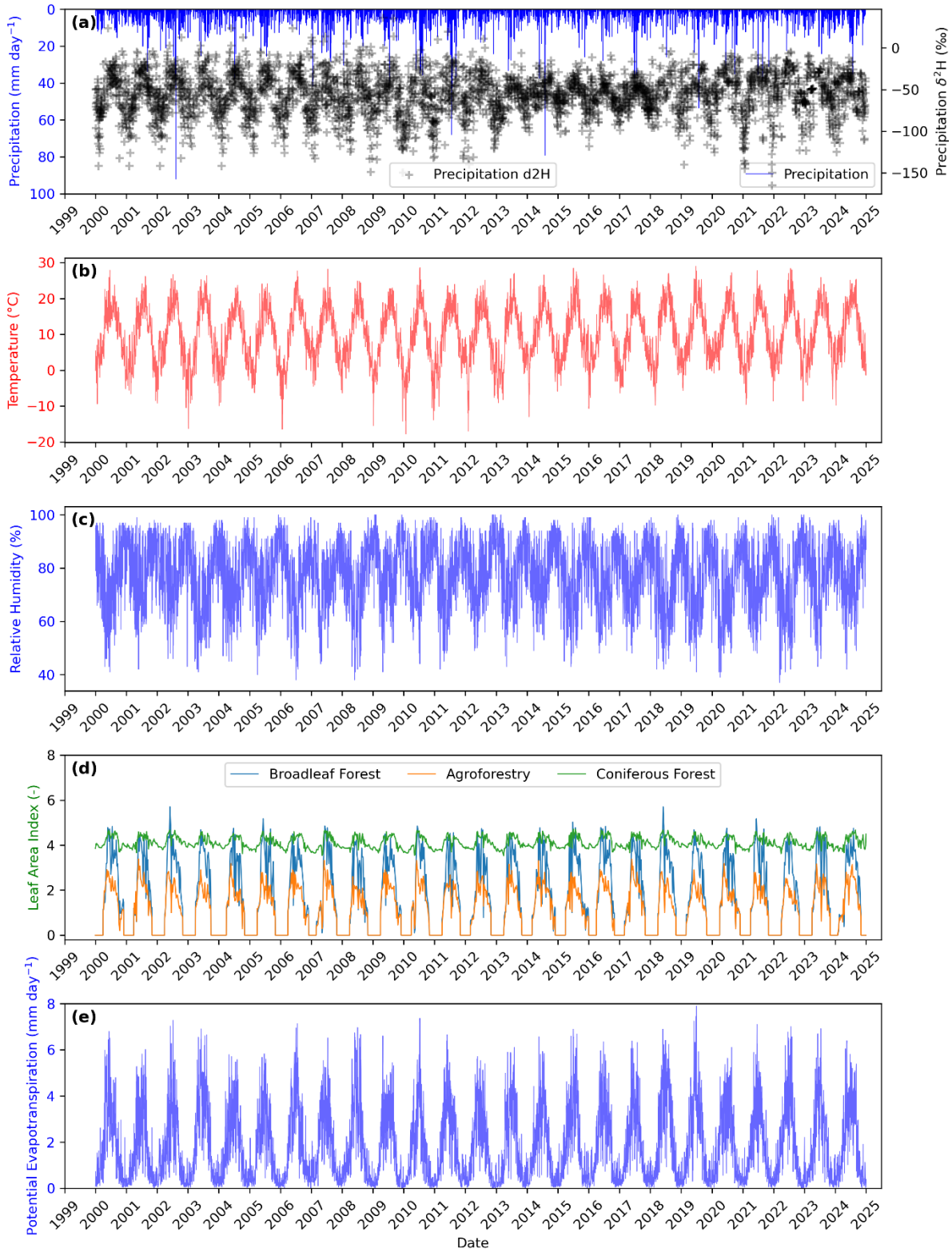

Figure S3. Input data for EcoPlot-iso long-term simulations (2000–2024) in the Demnitzer MillCreek Catchment: (a) Daily precipitation (mm day^{-1}) and precipitation δ^2H (‰); (b) Air temperature (°C); (c) Relative humidity (%); (d) Leaf Area Index (LAI); (e) Potential evapotranspiration (PET) (mm day^{-1}).

Table S2. Soil Moisture Measurement Devices and Aggregation Methods

Land Use Type	Device Type	Make / Model	Measurement Depths (cm)	Frequency	Aggregation Method
Surface Soil	Handheld soil moisture device	Theta handheld probe ML3 Sensor	0–10	Monthly	-
Subsurface Soil	Permanently installed probes	SMT-100, Umwelt-GeräteTechnik GmbH	Forest & Grassland: 20, 60, 100	15-minute intervals	Lower soil (10–30 cm): 20 cm Deeper soil (30–100 cm): mean (60 cm, 100 cm)
		CS650, Campbell Scientific	Agroforestry: 20, 40, 80		Lower soil (10–30 cm): 20 cm Deeper soil (30–100 cm): mean (40 cm, 80 cm)
			Cropland: 15, 40, 60, 100		Lower soil (10–30 cm): 15 cm Deeper soil (30–100 cm): mean (40 cm, 60 cm, 100 cm)

Table S3. EcoPlot-iso parameters, initial and calibrated parameters range for calibration. BF: Broadleaf Forest, CF: Conifer Forest, AF: Agroforest, GL: Grassland, CL: Cropland.

Parameter	Description	Sites	Initial range	Calibrated range		
				P5	Median	P95
rE	Radiation extinction factor (dimensionless)	BF	[-0.8, -0.5]	-0.79	-0.68	-0.54
		CF	[-0.8, -0.5]	-0.77	-0.61	-0.51
		AF	[-0.7, -0.3]	-0.69	-0.61	-0.46
		GL	[-0.5, -0.2]	-0.49	-0.45	-0.35
		CL	[-0.6, -0.3]	-0.59	-0.52	-0.39
α	Interception storage capacity parameter (mm per unit of LAI)	BF	[0.64, 0.84]	0.66	0.75	0.82
		CF	[1.00, 1.36]	1.02	1.15	1.33
		AF	[0.48, 0.84]	0.51	0.64	0.83
		GL	[0.32, 0.48]	0.33	0.4	0.47
		CL	[0.32, 0.48]	0.33	0.39	0.47
$S_{U,\,max}$	Maximum soil moisture content in the upper soil compartment (mm)	BF	[40, 60]	40.56	45.96	56.66
		CF		41.28	47.9	55.56
		AF		48.33	55.88	59.72
		GL		40.96	45.87	54.41
		CL		47.1	54.92	59.29
I_c	Soil infiltration capacity (mm/day)	BF	[40, 60]	40.95	48.89	58.67
		CF		41.06	50.43	58.94
		AF		41.1	50.34	58.96
		GL		40.36	46.62	58.37
		CL		40.94	49.85	58.42
k_{s1}	Saturated hydraulic conductivity of the upper soil compartment (mm/day)	BF	[5, 20]	5.3	9.81	18.02
		CF		5.32	10.65	18.19
		AF		6.13	10.83	17.79
		GL		5.81	10.43	18.82
		CL		7.23	13.25	18.65
k_{s2}	Saturated hydraulic conductivity of the middle soil compartment (mm/day)	BF	[3, 15]	4.13	8.39	14.54
		CF		3.28	7.6	12.98
		AF		3.48	6.88	13.92
		GL		3.28	7.9	14.08
		CL		3.4	6.47	13.43
k_{s3}	Saturated hydraulic conductivity of the deep soil compartment (mm/day)	BF	[1, 10]	2.25	5.59	8.95
		CF		3.07	6.47	9.65
		AF		1.45	5.06	9.38
		GL		1.42	4.08	8.79
		CL		2.27	6.27	9.57
$S_{M,\,max}$	Maximum soil moisture content in the middle soil compartment (mm)	BF	[50, 100]	51.65	60.28	91.35
		CF		52	64.96	96.12
		AF		52.32	64.64	90.33
		GL		51.06	61.42	91.05
		CL		51.08	69.57	94.22
$S_{D,\,max}$	Maximum soil moisture content in the deep soil compartment (mm)	BF	[150, 250]	153.1	191.47	242.03
		CF	[30, 50]	32.82	41.9	49.13
		AF	[250, 450]	258.21	319.64	420.76
		GL	[100, 300]	116.11	169.03	286.46
		CL	[250, 450]	270.24	345.34	436.47
g_1	Nonlinear scaling parameter for the upper soil compartment	BF	[1, 5]	2.24	3.48	4.88
		CF		3.07	4.26	4.92
		AF		2.51	4	4.82
		GL		2.26	3.72	4.86
		CL		2.56	3.8	4.86
g_2	Nonlinear scaling parameter for the middle soil compartment	BF	[1, 5]	1.71	3.16	4.86
		CF		1.33	2.65	4.52
		AF		1.71	3.15	4.76
		GL		1.33	2.71	4.62

		CL		1.22	2.74	4.62
g_3	Nonlinear scaling parameter for the deep soil compartment	BF	[1, 5]	1.13	2.37	4.38
		CF		2.76	3.84	4.83
		AF		1.37	3.25	4.82
		GL		1.12	1.88	4.13
		CL		2.67	3.96	4.91
PF_{Scale}	Preferential flow path parameter (dimensionless)	BF	[0.1, 0.6]	0.25	0.47	0.58
		CF		0.12	0.25	0.34
		AF		0.13	0.3	0.53
		GL		0.17	0.35	0.55
		CL		0.14	0.31	0.55
IntSp	Passive interception storage mixing volume (mm)	BF	[0.5, 1]	0.52	0.68	0.94
		CF		0.54	0.75	0.98
		AF		0.51	0.75	0.96
		GL		0.52	0.77	0.99
		CL		0.52	0.73	0.96
StoSo	Passive upper soil storage mixing volume (mm)	BF	[1, 20]	7.26	12.9	18.98
		CF		1.9	9.88	19.2
		AF		1.12	4.29	8.4
		GL		1.24	4.78	9.75
		CL		1.31	3.35	8.18
gwSp	Passive middle soil storage mixing volume (mm)	BF	[3, 40]	3.97	9.81	22.06
		CF		16.6	25.14	36.02
		AF		5.46	12.9	22.87
		GL		3.47	10.75	20.85
		CL		7.21	16.86	28.86
lowSP	Passive deep soil storage mixing volume (mm)	BF	[10, 100]	59.59	88.97	99.4
		CF		20.45	39.2	77.04
		AF		15.2	43.24	87.19
		GL		24.7	58.06	92.59
		CL		12.06	28.81	65.93
k	Seasonality factor in the Craig-Gordon model (dimensionless)	BF	[0.25, 0.9]	0.27	0.55	0.82
		CF		0.33	0.6	0.85
		AF		0.29	0.6	0.86
		GL		0.29	0.62	0.87
		CL		0.37	0.69	0.89
x	Water vapor mixing ratio in the Craig-Gordon model (dimensionless)	BF	[0.25, 0.75]	0.28	0.55	0.72
		CF		0.3	0.53	0.71
		AF		0.29	0.49	0.72
		GL		0.27	0.46	0.7
		CL		0.27	0.42	0.69
β	Root distribution factor (m^{-1})	BF	[0, 2]	0.05	0.39	1.09
		CF		0.88	1.51	1.93
		AF		0.02	0.25	0.63
		GL		0.02	0.38	1.42
		CL		0.13	0.74	1.47

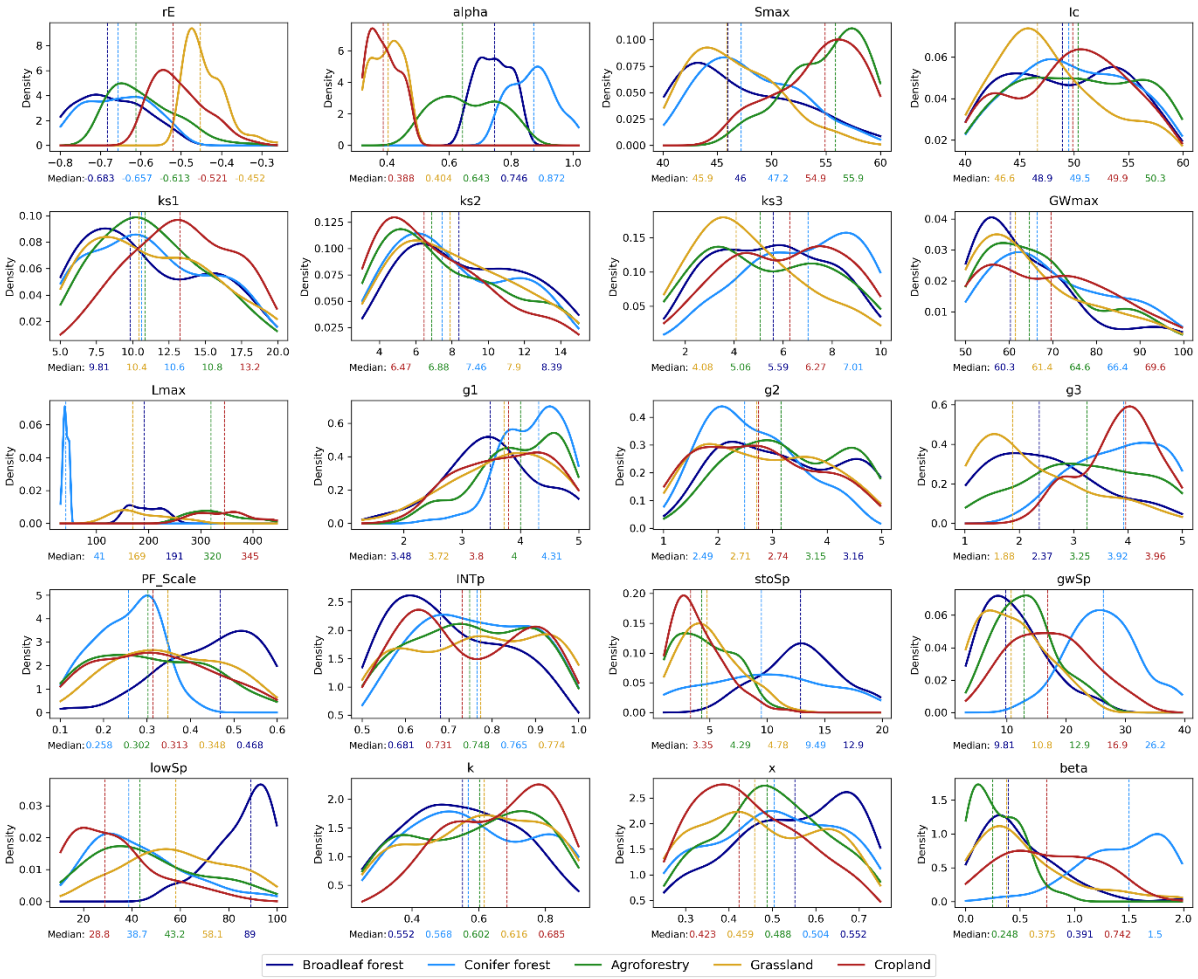

Figure S4. Probability density distributions of the 20 calibrated ecohydrological parameters for five land-use types (broadleaf forest, conifer forest, agroforestry, grassland, and cropland) based on 100 behavioural simulations from the EcoPlot-iso model. Each panel represents one parameter, with kernel density estimates (KDEs) shown in different colours corresponding to each land-use type. Vertical dashed lines indicate the median values of the posterior parameter distributions. Below each subplot, the median values are listed in ascending order (left to right) with text colours matching the respective land-use type. The density plots highlight parameter sensitivities and the distinct parameterization patterns across contrasting vegetation covers.

Table S4. Kling–Gupta Efficiency (KGE) values for soil moisture and soil water isotopes (δ^2H), comparing observed and mean simulated values at each land use site. Soil moisture KGE values are reported for both the calibration and validation periods, whereas soil water isotope KGE values are shown for the calibration period only due to limited isotope observations. The calibration and validation periods are 2000–2021 and 2022–2024 for broadleaf, conifer forest and agroforestry sites, and 2000–2022 and 2023–2024 for cropland and grassland sites, respectively.

Sites	Soil moisture – Calibration period			Soil moisture – Validation period		Soil water isotope (δ^2H) – Calibration period		
	Upper	Lower	Deep	Lower	Deep	Upper	Lower	Deep
Broadleaf Forest	0.57	0.76	0.85	0.73	0.83	0.63	0.74	0.70
Conifer forest	0.61	0.62	0.61	0.73	0.78	0.77	0.81	0.53
Agroforestry	0.72	0.77	0.74	0.80	0.76	0.82	0.84	0.79
Grassland	0.89	0.75	0.78	0.65	0.53	0.71	0.76	0.62
Cropland	0.53	0.64	0.77	0.54	0.41	0.83	0.85	0.37

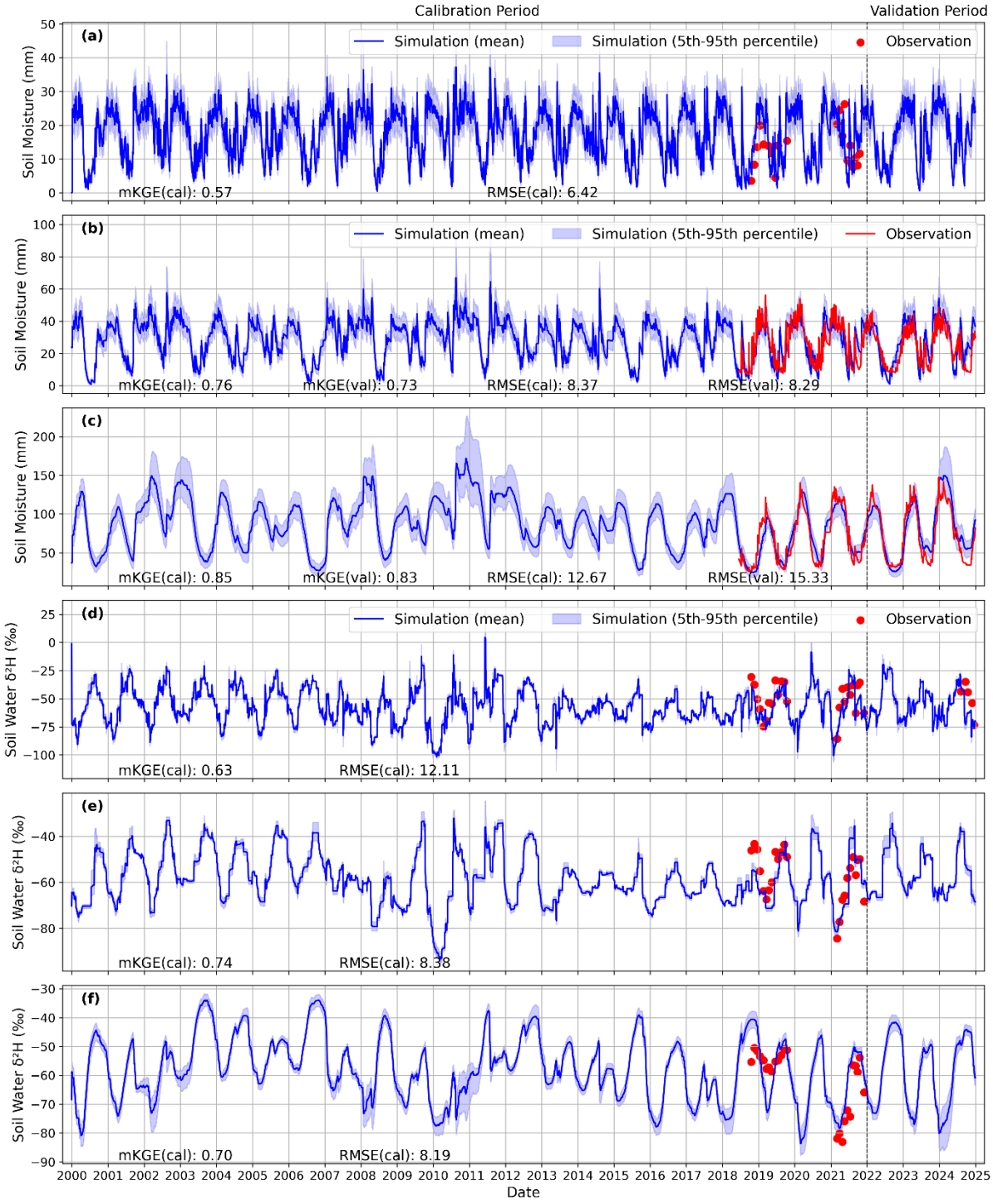

Figure S5. Observed and simulated soil moisture and soil water stable isotope dynamics for the broadleaf forest site. Panels (a–c) show soil moisture time series for the upper (0-10 cm), middle (10-30 cm), and deep (30-100 cm) soil layers, while panels (d–f) show the corresponding soil water δ²H for the same layers. Solid blue lines indicate the ensemble mean of the simulations (n = 100), and the shaded bands represent the 5th–95th percentile range. Red symbols or lines denote observations. The vertical dashed line marks the separation between the calibration period (2000–2021) and the validation period (2022–2024). Model performance is quantified using the modified Kling–Gupta efficiency (mKGE) and root mean square error (RMSE), reported separately for the calibration period in all panels and for the validation period in the middle and deep soil moisture layers, where observations are available.

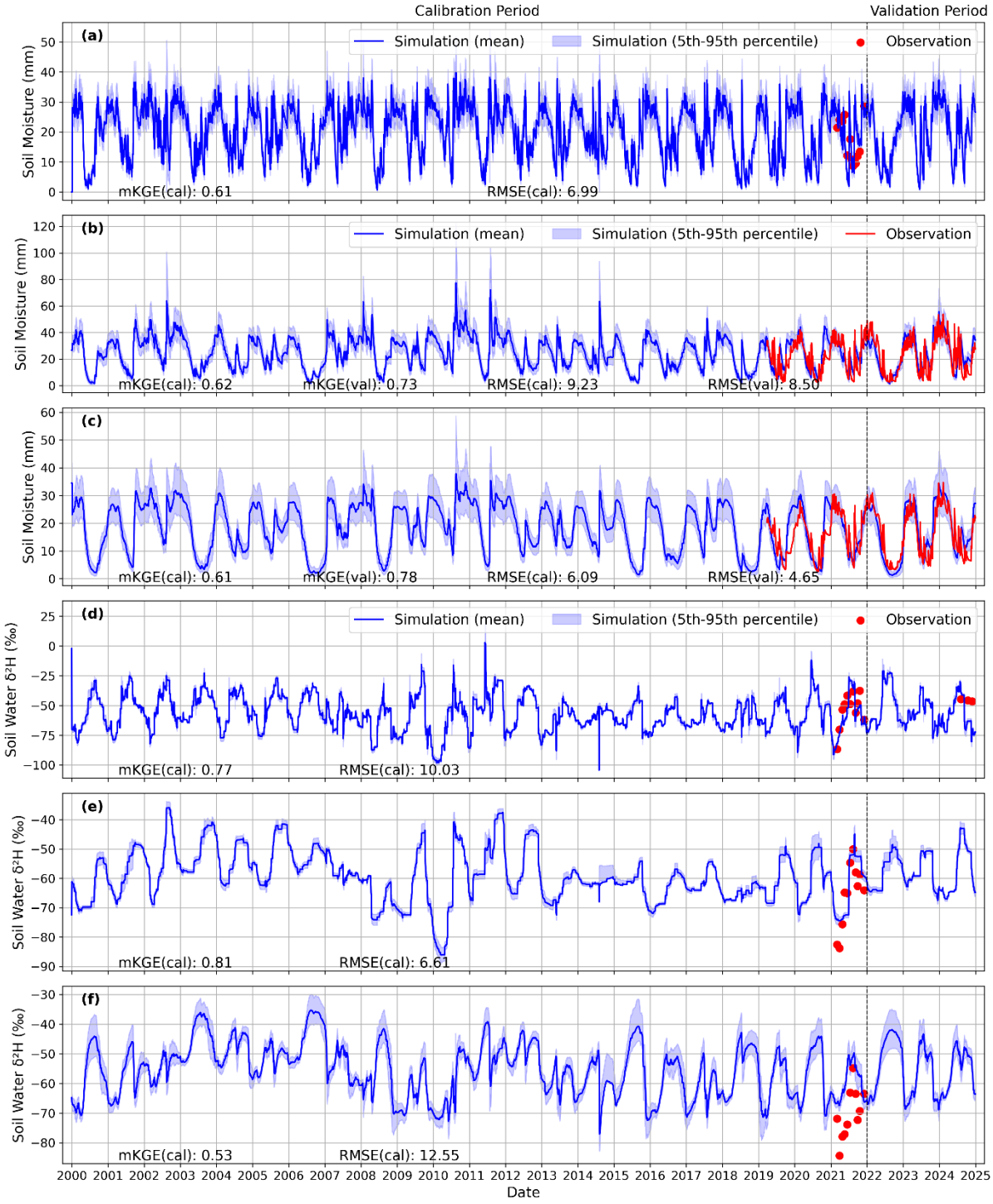

Figure S6. Observed and simulated soil moisture and soil water stable isotope dynamics for the conifer forest site. Panels (a–c) show soil moisture time series for the upper (0-10 cm), middle (10-30 cm), and deep (30-100 cm) soil layers, while panels (d–f) show the corresponding soil water δ²H for the same layers. Solid blue lines indicate the ensemble mean of the simulations (n = 100), and the shaded bands represent the 5th–95th percentile range. Red symbols or lines denote observations. The vertical dashed line marks the separation between the calibration period (2000–2021) and the validation period (2022–2024)**.** Model performance is quantified using the modified Kling–Gupta efficiency (mKGE) and root mean square error (RMSE), reported separately for the calibration period in all panels and for the validation period in the middle and deep soil moisture layers, where observations are available.

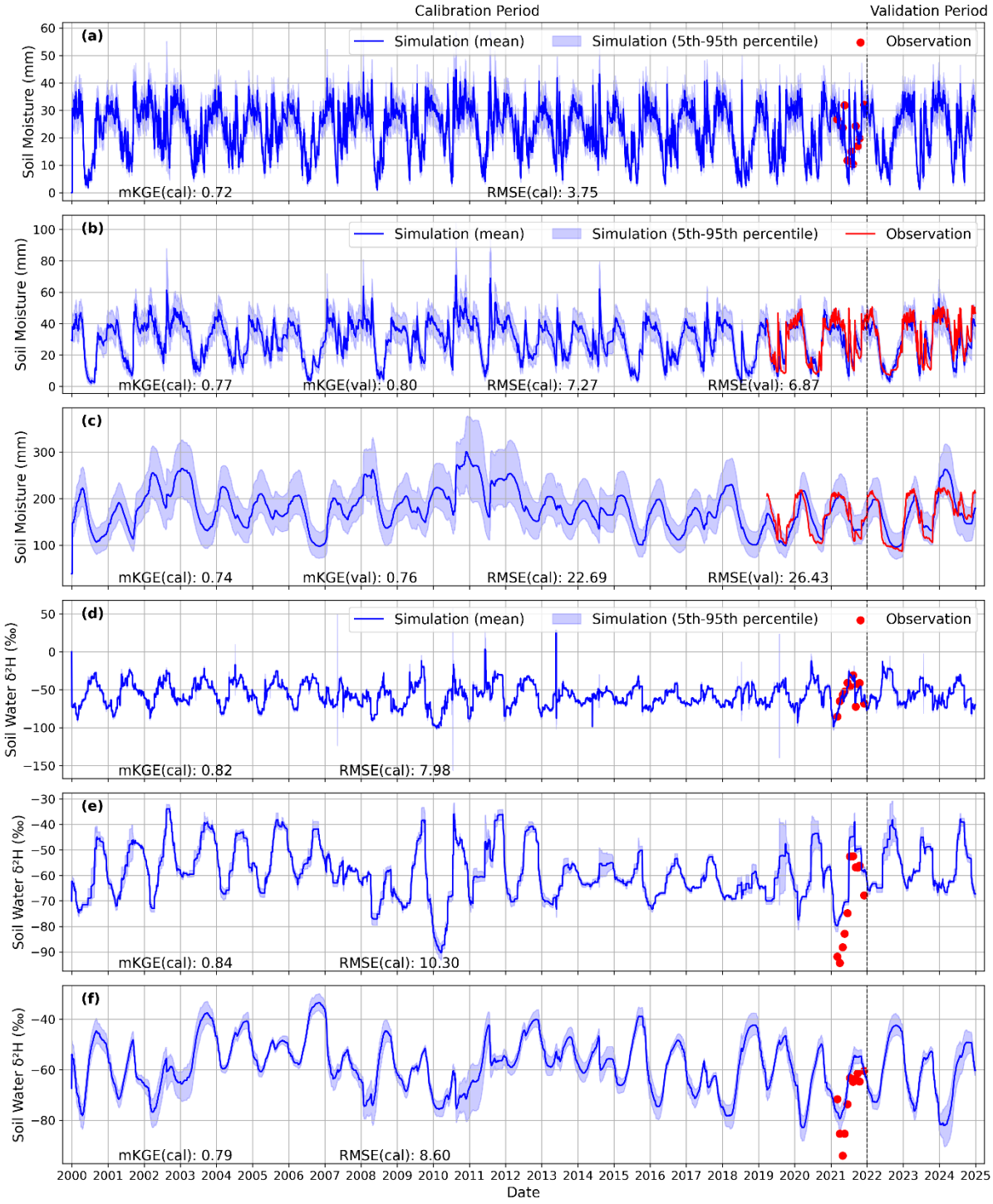

Figure S7. Observed and simulated soil moisture and soil water stable isotope dynamics for the agroforestry site. Panels (a–c) show soil moisture time series for the upper (0-10 cm), middle (10-30 cm), and deep (30-100 cm) soil layers, while panels (d–f) show the corresponding soil water δ^2H for the same layers. Solid blue lines indicate the ensemble mean of the simulations (n = 100), and the shaded bands represent the 5th–95th percentile range. Red symbols or lines denote observations. The vertical dashed line marks the separation between the calibration period (2000–2021) and the validation period (2022–2024)**.** Model performance is quantified using the modified Kling–Gupta efficiency (mKGE) and root mean square error (RMSE), reported separately for the calibration period in all panels and for the validation period in the middle and deep soil moisture layers, where observations are available.

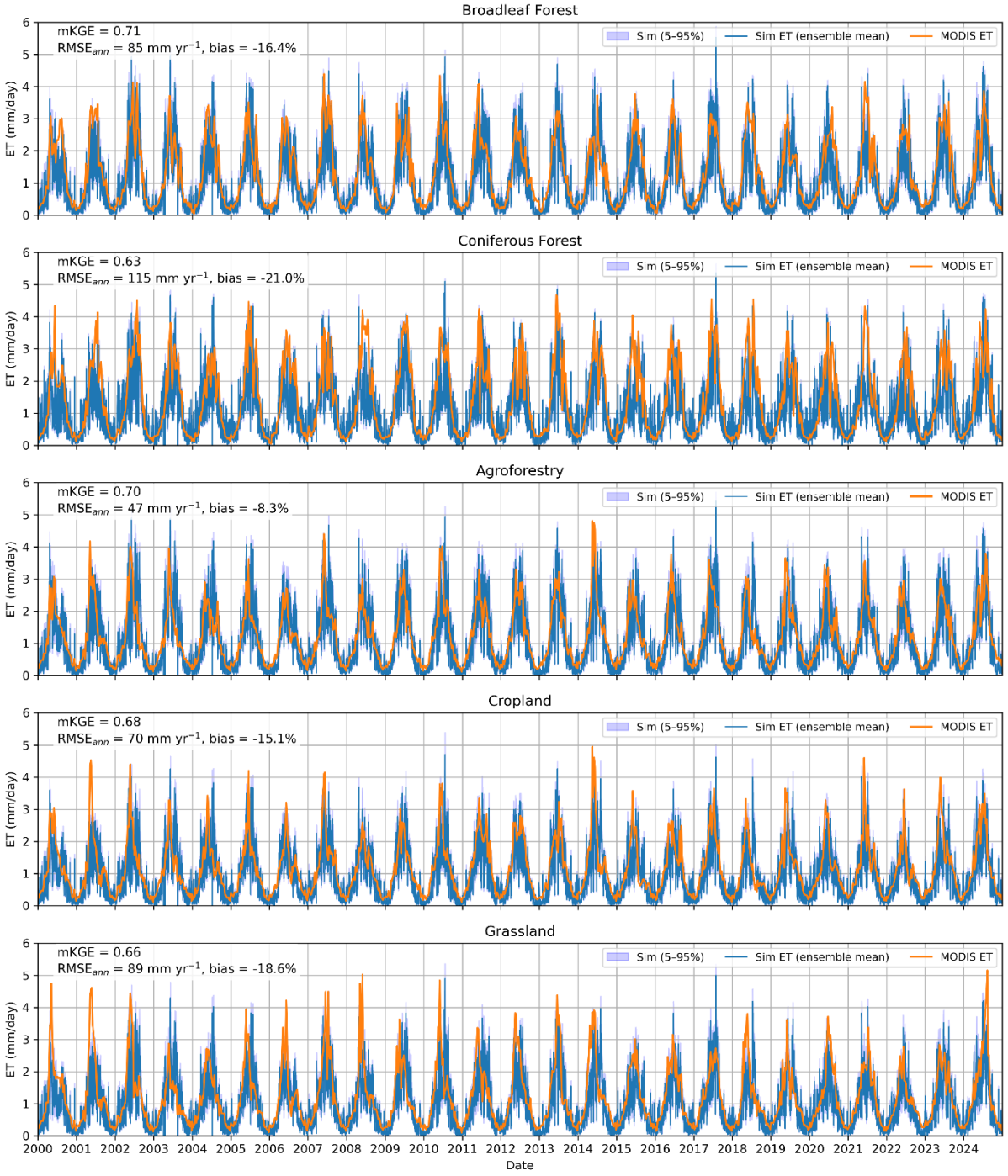

Figure S8. Comparison of simulated and MODIS-derived evapotranspiration (ET) for five land-use types (Broadleaf Forest, Coniferous Forest, Agroforestry, Cropland, and Grassland) over the period 2000–2024. Solid blue lines show the ensemble mean of simulated daily ET across 100 model simulations, while the shaded blue envelope indicates the 5th–95th percentile range. Orange lines denote observed daily ET derived from MODIS. Model performance is quantified using the mean Kling–Gupta Efficiency (Kling et al., 2012) calculated from daily ET across the 100 simulations, , together with the root mean square error of annual ET sums (RMSE; mm yr^{-1}) and the relative bias of annual ET sums (%). Performance metrics shown in each panel represent ensemble averages across all simulations.

Table S5. Performance of simulated evapotranspiration (ET) against MODIS-derived ET for five land-use types (Broadleaf Forest, Coniferous Forest, Agroforestry, Cropland, and Grassland) over the period 2000–2024. Model skill is evaluated using the Kling–Gupta Efficiency (Kling et al., 2012) computed from daily ET time series, together with the root mean square error of annual ET sums (RMSE; mm yr^{-1}) and the relative bias of annual ET sums (%). Annual ET sums were derived from daily ET for each of the 100 EcoPlot-iso ensemble simulations and compared against MODIS observations. Reported values represent ensemble statistics across the 100 simulations for each land-use type.

Sites	Evapotranspiration		
	KGE	RMSE (mm yr^{-1})	Relative bias of annual ET sums (%)
Broadleaf Forest	0.71	85	-16.4
Conifer forest	0.63	115	-21.0
Agroforestry	0.70	47	-8.3
Grassland	0.68	70	-15.1
Cropland	0.66	89	-18.6

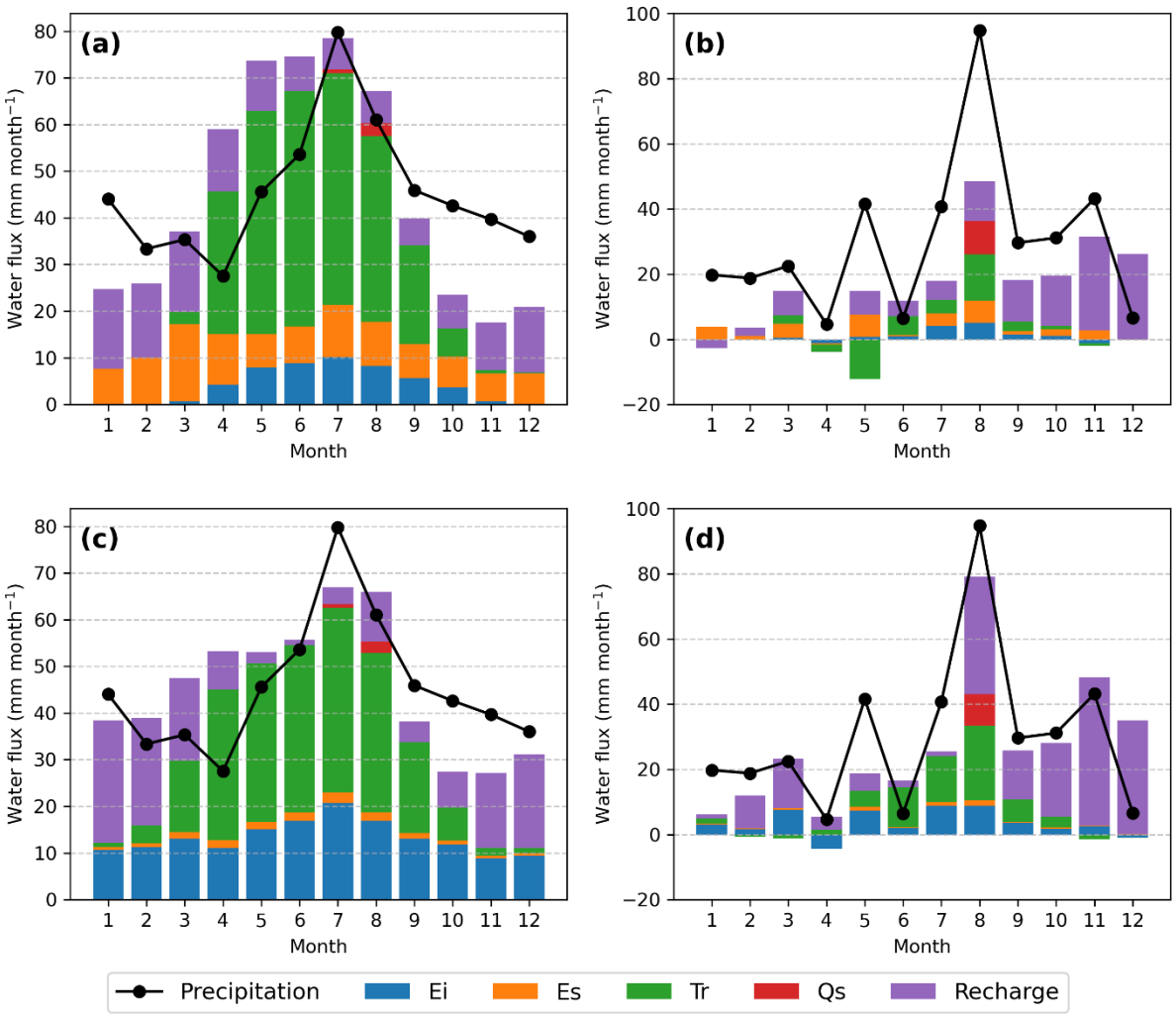

Figure S9. Mean monthly water balance components for agroforestry and conifer forest sites in the Demnitzer Millcreek catchment over the period 2000–2024, simulated with EcoPlot-iso using the mean of the 100 best-performing parameter sets (see Section 3.4). Stacked bars show monthly totals of interception evaporation (Ei), soil evaporation (Es), transpiration (Tr), surface runoff (Qs), and groundwater recharge, while the black line indicates precipitation (P). Panels show (a, c) long-term mean monthly water balance (mm month⁻¹) and (b, d) differences between wet years (2002, 2007, 2010, 2023) and dry years (2006, 2018, 2022), expressed as wet minus dry (mm month⁻¹).

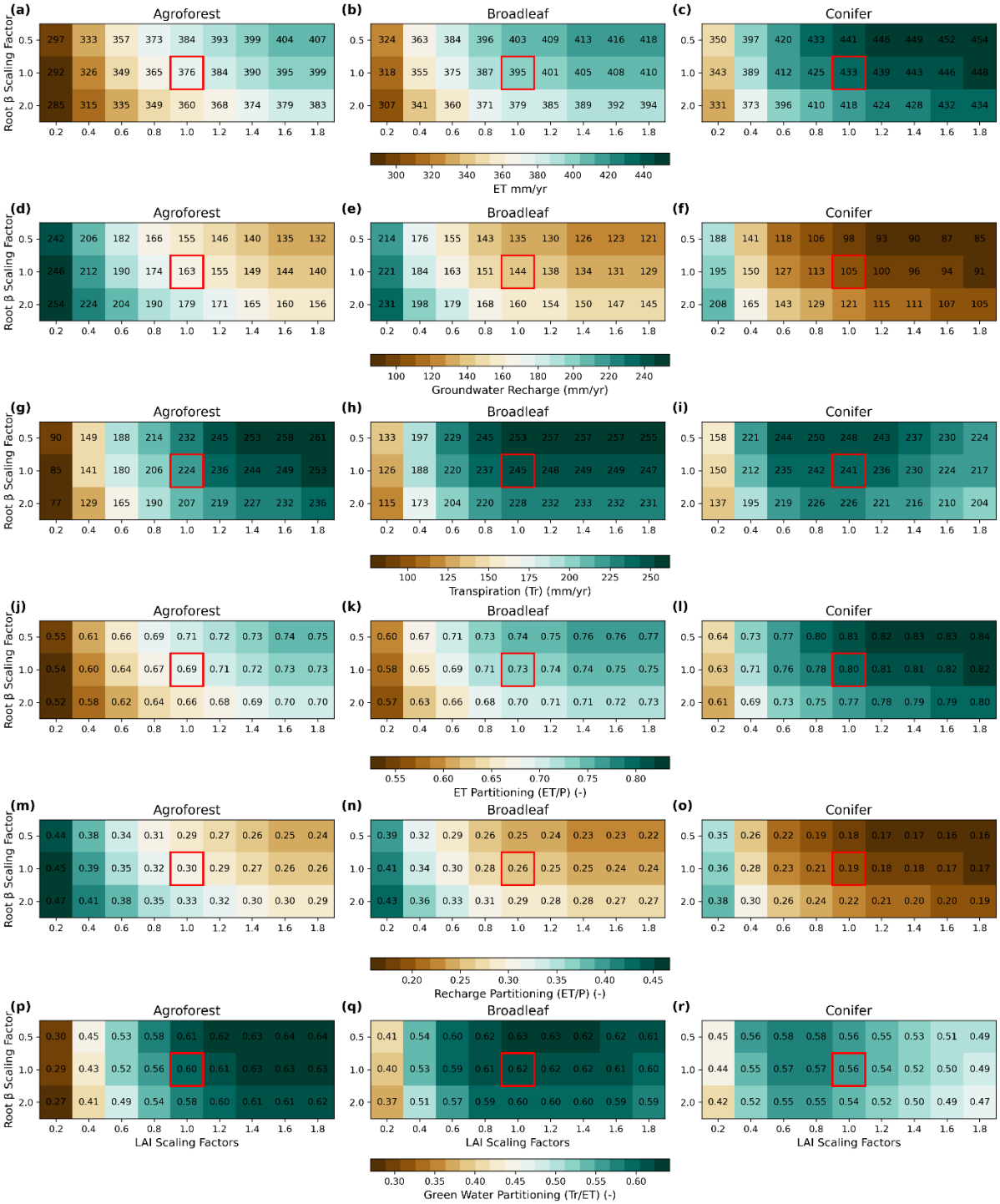

Figure S10. Green and blue water partitioning across forest types, LAI scaling factors, and root distributions. The heatmaps illustrate evapotranspiration (ET) (a–c), groundwater recharge (d–f), transpiration (Tr) (g–i), ET partitioning (ET/P) (j–l), and green water partitioning (Tr/ET) (m–o) for three forest types (Agroforest, Broadleaf, and Conifer). The x-axis represents scaling factors (forest density), while the y-axis represents scaled root parameter β (0.5×β, 1×β, and 2×β, where β is the site-calibrated root parameter). Each heatmap includes numeric values for clarity, with red-outlined cells indicating the baseline simulations (Broadleaf forest, LAI scaling factor = 1 and β=1×β).

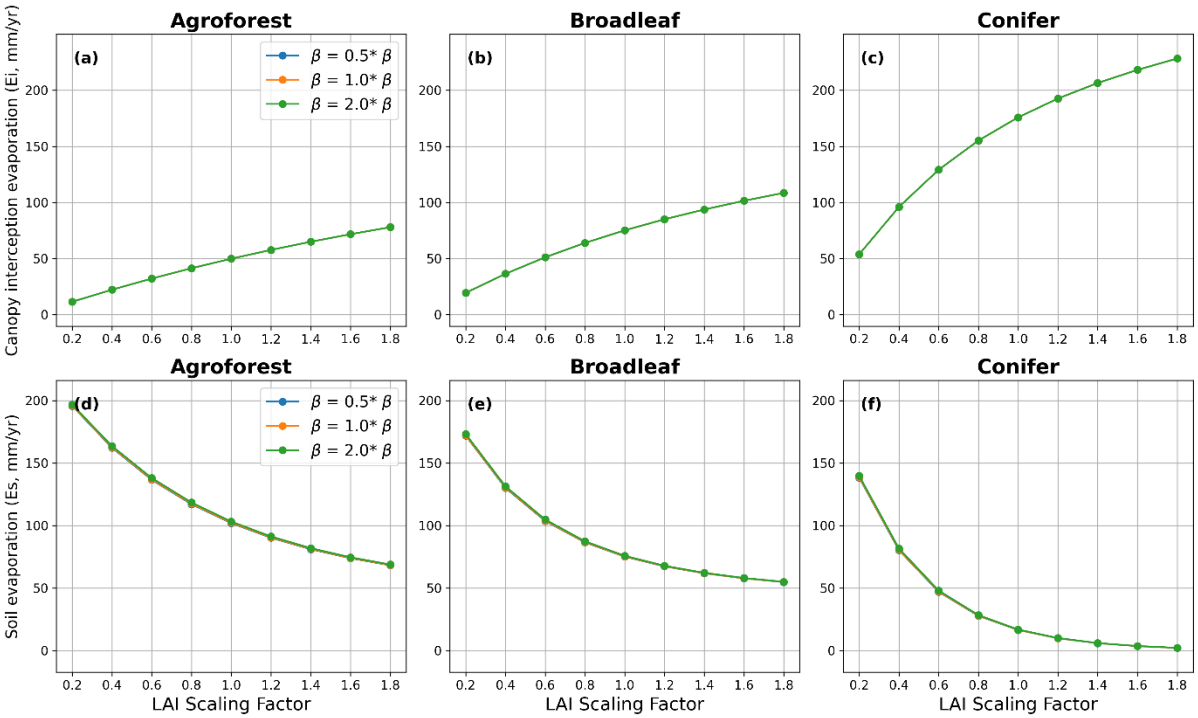

Figure S11. Annual mean evaporation components from (a)–(c) the canopy (Ei) and (d)–(f) the soil surface (Es) across different forest types (Agroforest, Broadleaf, Conifer) and LAI scaling factors. Lines indicate results for different root parameter (β values).

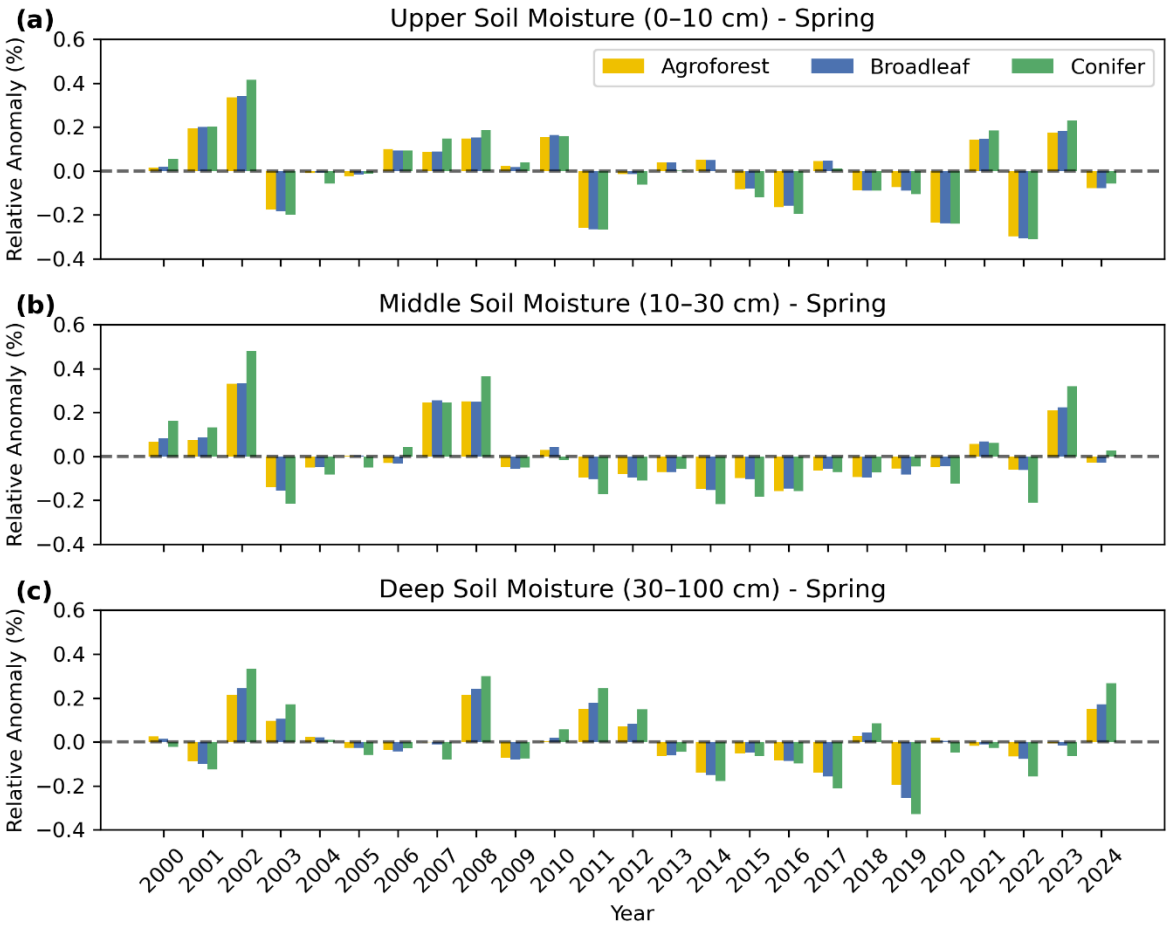

Figure S12. Relative soil moisture anomalies for spring (March–May) across three soil layers: (a) surface (0–10 cm), (b) lower layer (10–30 cm), and (c) deep layer (30–100 cm) for three forest types (Agroforest, Broadleaf, Conifer).

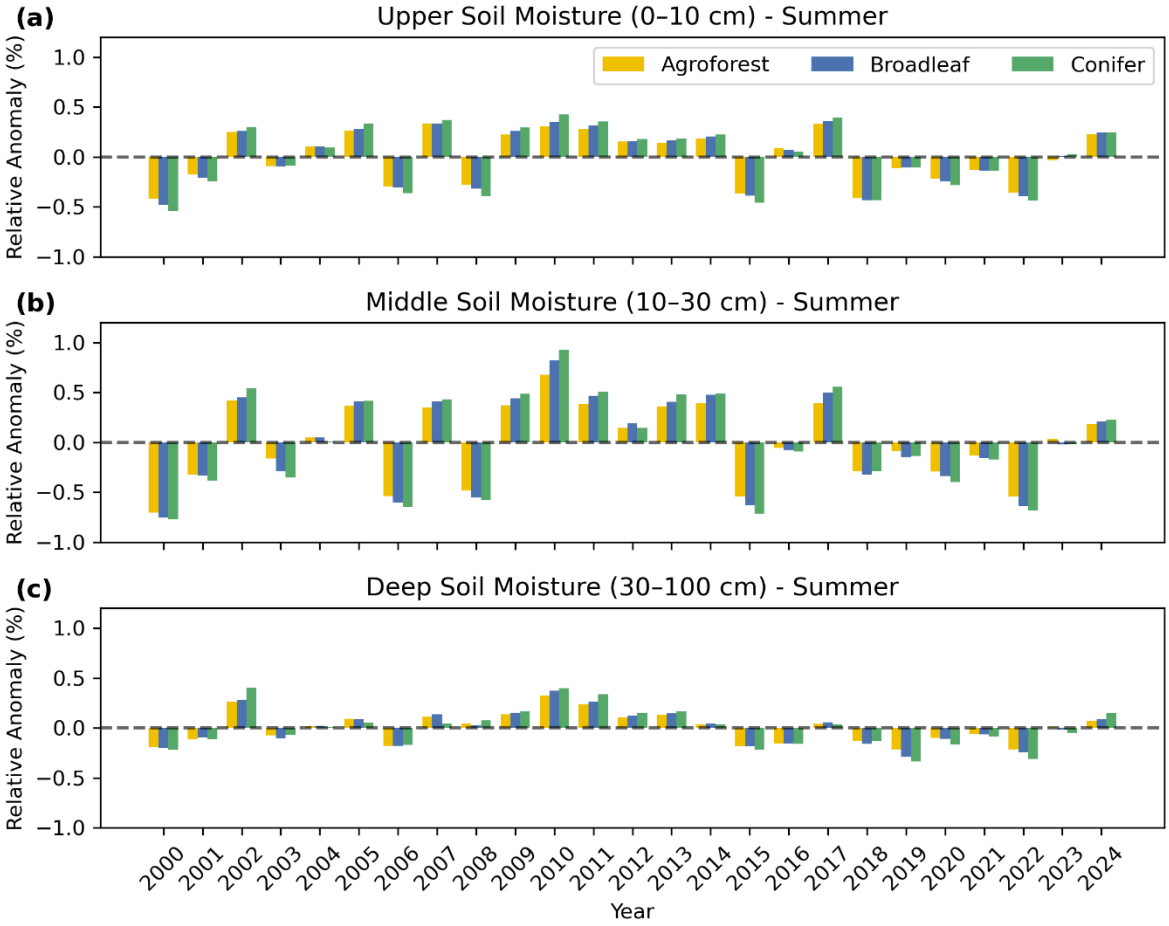

Figure S13. Same as Figure 11 but for forests with a shallow root system (root parameter β = 2.0* β).

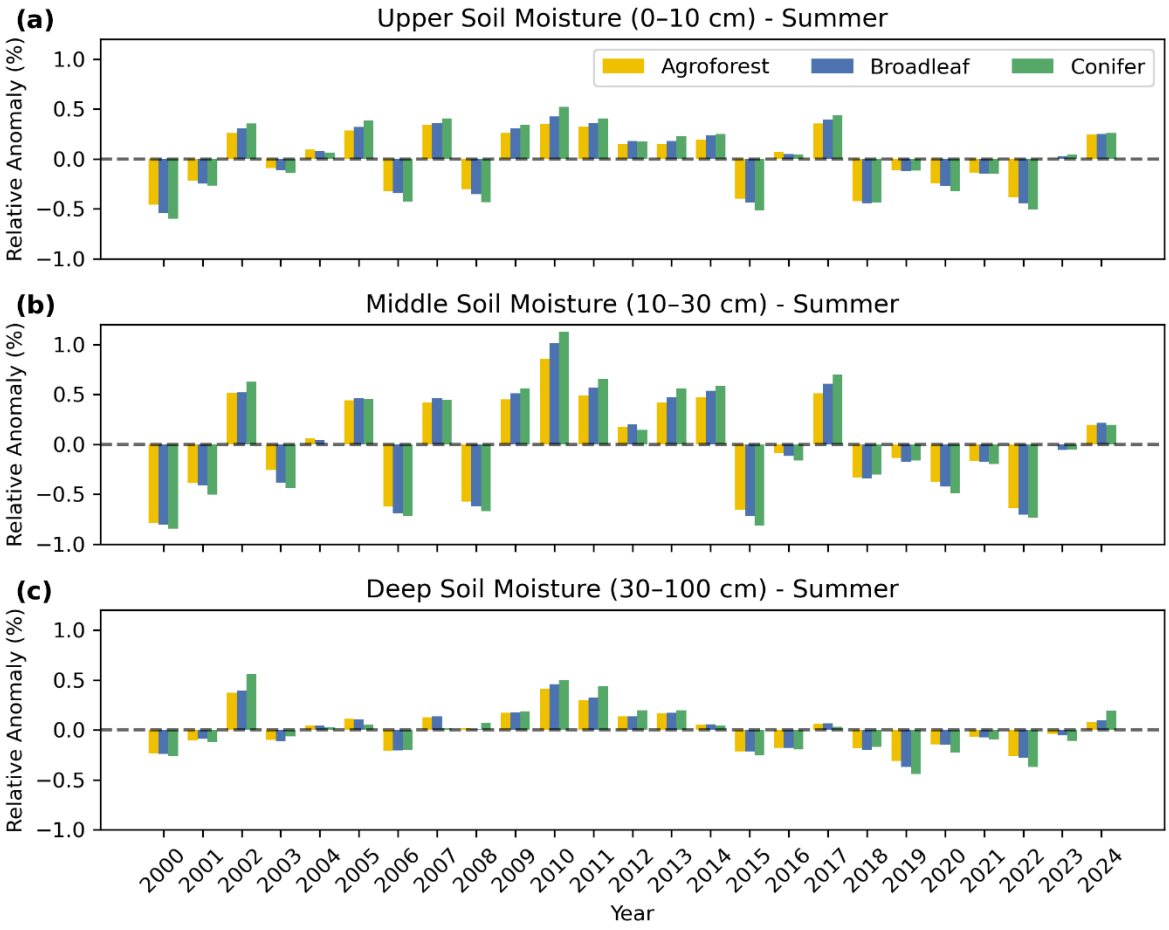

Figure S14. Same as Figure 11 but for forests with a higher density (LAI scaling factor = 1.6).